Results in Control and Optimization 13 (2023) 100325

Contents lists available at ScienceDirect

Results in Control and Optimization

journal homepage: www.elsevier.com/locate/rico

Modeling and optimal control of the transmission dynamics of amebiasis

Stephen Edward [a,*], Godfrey Edward Mpogolo [b]

[a] Department of Mathematics and Statistics, University of Dodoma, Box 338, Dodoma, Tanzania
[b] Department of Management Studies, Tanzania Institute of Accountancy, Box 9522, Dar es Salaam, Tanzania

ARTICLE INFO

Keywords:
Optimal control
Intestinal amebiasis
Awareness programs
Sanitation
Medical treatment
Diarrhea

ABSTRACT

In this paper, the mathematical models for amebiasis are developed and presented. The first model considers the transmission dynamics of amebiasis coupled with two constant controls: treatment and sanitation. The next-generation matrix calculates the effective reproductive number, which is then used to assess model system stability. A sensitivity analysis is performed to determine the primary factors affecting disease transmission. Nonetheless, the results suggest that indirect transmission is more crucial than direct transmission in spreading disease. In addition, we extended the first model to incorporate time-dependent optimal control measures, namely community awareness, treatment, and sanitation. The aim was to reduce the number of infections emanating from interaction with carriers, infected people, and polluted environments while minimizing the expenses associated with adopting controls. The optimal control problem is solved by applying Pontryagin's Maximum Principle and forward and backward-in-time fourth-order Runge–Kutta methods. The results indicate that an awareness program is optimal when a single control strategy is the only available option. However, when a combination of two controls is implemented, an approach combining awareness programs and treatment is shown to be optimal. Generally, the best strategy is implementing a combination of all three controls: awareness programs, sanitation, and treatment.

1. Introduction

Amebiasis is a gastrointestinal illness caused by an infestation with the one-celled parasite called *Entamoeba histolytica*. The disease is characterized by loose stools containing blood and mucus within the intestines, commonly known as amoebic diarrhea. This particular gastrointestinal parasite disease is widely observed among the human population, resulting in an annual incidence of over 50 million new infections and causing more than 100,000 fatalities globally. *Entamoeba* comprises three morphologically indistinguishable species, including *Entamoeba histolytica*, which is pathogenic and associated with disease, along with two non-pathogenic variants namely *Entamoeba dispar* and *Entamoeba Moshkovskii* [1–4]. According to [5], amebiasis remains a severe public health problem in places marked by a dense population, poor hygiene, and financial restrictions, especially in tropical and subtropical climates. In advanced countries, amebiasis affects older people more frequently than younger people. It is also prone to affect men who have experienced sexual relations with other men or who live in institutionalized environments. However, in tropical areas, the prevalence of amebiasis is different and affects the general population, especially those seeking treatment for diarrhea in healthcare centers. Therefore, it is crucial to comprehend the epidemiology of this disease in tropical regions where it causes the most illness and

* Corresponding author.
E-mail addresses: stephen.edward@udom.ac.tz (S. Edward), godfrey.mpogolo@tia.ac.tz (G.E. Mpogolo).

https://doi.org/10.1016/j.rico.2023.100325
Received 8 January 2023; Received in revised form 1 October 2023; Accepted 22 October 2023
Available online 28 October 2023

death [6]. Additionally, *Entamoeba histolytica* can avoid detection and cause damage to other internal human organs like the liver, lungs, and brain. Amebiasis is a persistent and disfiguring infection under the Neglected Tropical Diseases (NTDs) classification [7]. The clinical presentation of the disease presents a spectrum of symptoms, ranging from asymptomatic colonization to onset of amebic colitis, marked by diarrhea, and invasive extraintestinal amebiasis, frequently leading to the development of liver abscesses [8].

According to the work by [4,6], an incubation period can last from a few days to several years after being infected with amebiasis. Typically, the incubation period lasts between 1 to 4 weeks. After this period, the infected individual may develop either an asymptomatic (latent) stage or an acute stage of amebiasis colitis. Mature cysts of Entamoeba histolytica are resistant and can survive for several weeks in soil, 12 days in cool and damp conditions, and up to 30 days in water. They are also able to withstand temperatures ranging from 50 °C to 40 °C. The development of symptoms in infected individuals depends on their immune system and other unknown biochemical factors of the parasite and the host. Approximately 90% of people infected with Entamoeba histolytica will experience asymptomatic amebiasis, while the remaining 10% will exhibit amebiasis colitis symptoms [6]. Amebiasis occurs after ingesting Entamoeba histolytica cysts spread through polluted food or beverages. Once the infection reaches the large intestine, it transforms from a cyst to an invasive trophozoite through cellular division and multiplication [9].

Metronidazole and similar compounds derived from nitroimidazole are commonly used to treat invasive parasitic infections. However, these drug therapies are associated with undesirable side effects, costly, and not readily accessible in some countries or regions [10]. Enhancing water purification systems and promoting better hygiene practices has the potential to reduce disease incidence, but it would demand significant time, policy reforms, and financial investments. As a result, an appealing option could be the development of a vaccine and the implementing of vaccination programs in developing nations. There has been no approval for human clinical trials of a vaccine against amebiasis. However, promising findings have emerged from recent studies on vaccine development [11].

A vast of literature on *Entamoeba histolytica* is from medical, clinical, or other related fields. However, there are very few mathematical works have been done so far to understand the transmission dynamics of amebiasis, such as those by [7,12,13]. The scholars [12] formulated a mathematical framework: susceptible–exposed–infectious–recovered (SEIR) with a slight modification of including a carrier-class. This is one of the earliest models developed for amebiasis so far. Also, [7] contributed to the work of [12] by analyzing their model. The study by [12] was expanded upon by [13], who conducted an in-depth mathematical analysis of the model and solved the problem raised numerically.

Optimal control is a mathematical discipline that seeks the most effective means of controlling a dynamical system. Innumerable fields, such as biomedical sciences, economics, physical science, and engineering, have extensively used the theory (Lenhart & Workman 2002) [14]. The objective of optimal control in epidemics is to seek, amongst existing options, the most effective one that minimizes the incidence rate while optimizing the cost of deploying a strategy to control the progression of the disease. Several researchers, such as [15–22], have employed optimal control theory to describe intervention strategies. Using optimal control theory, they demonstrated the substantial role played by control measures (e.g. education, treatment, vaccination, quarantine, social distancing, face-mask usage in public, use of Personal Protective Equipment (PEP), e.t.c.) in halting the disease's progression.

Moreover, [23] investigated cholera via double control measures: educational awareness and water chlorination. A cost–benefit analysis determined that educational awareness was the most cost-effective method for preventing the outbreak. A study by [24] established a compartmental model for cholera integrating vaccination, treatments, and water sanitation. The optimal control theory was then applied to find a cost-effective solution for numerous time-dependent cholera interventions. Furthermore, [25] researched effective control techniques for dysentery. They concluded that sanitation and education was the most effective and cost-effective strategy.

Several mathematical works, such as those by [7,12,13], have investigated the dynamics of amebiasis. Nevertheless, the existing literature primarily overlooks the impact of environmental pathogens and effective control measures on amebiasis transmission. Hence, it becomes crucial to develop a mathematical model that integrates the effect of environmental pathogens on the transmission dynamics of amebiasis and optimal strategies for epidemic control.

The rest of the paper is structured as follows: In Section 2, we will go through how to develop and analyze a model, and in Section 3, we will jump more deeply into the sensitivity analysis. The formulation of an optimization problem and analysis is given in Section 4. Next, numerical simulation is presented in Section 5, and Section 6 finalizes the paper with concluding remarks.

2. Model formulation and analysis

The first part of this paper is derived from the work by [26] posted as a preprint. This study extends the findings of [13] by introducing a new compartment to account for the pathogen reservoir in the surroundings. As a result, the upgraded model will incorporate two transmission pathways: direct transmission between individuals and indirect transmission from the surroundings to individuals. This contrasts with previous studies [7,12,13], which concentrated on direct transmission as the only transmission mode. Additionally, in contrast to earlier studies, the present model includes two control measures, namely treatment and sanitation, among the interventions to mitigate the transmission and spread of amebiasis. In the later section, the study will include awareness campaigns as an additional control strategy. Five different and separate epidemiological populations collectively make up the entire human population: those considered vulnerable $S(t)$; those who have been exposed $E(t)$; those who are proactively infected $I(t)$, those who are carrying the pathogen devoid of exhibiting signs and symptoms $C(t)$, and those who have made a full recovery $R(t)$. The $SEIR$ model is modified by adding the carrier compartment $C(t)$, as evidence suggests that 90% of infected cases remain asymptomatic (see [6]). Pathogens need reservoirs, which can be living organisms or non-living sites like soil and water, to persist

Table 1
Parameters and their description.

Parameter	Description	Value	Source
Λ	Rate of recruitment of individuals into the susceptible class	469 Humans/year	[24]
α_1	Transmission rate for infectious individuals	0.6/year	[13]
α_2	Transmission rates for carriers	1/3/year	[31]
α_3	Effective transmission rate of amebiasis due to the environment to human interaction	0.4465/year	[3]
δ	Incubation rate (Rate at which exposed individuals, $E(t)$ progress to either class $I(t)$ or $C(t)$)	1/28/day	[4,15]
μ	Natural human mortality rate	1/50/year	[31]
d_1	Disease induced death rate by $I(t)$	0.02/year	Assumed
d_2	Disease induced death rate by $C(t)$	0.03/year	Assumed
η_1	Recovery rate of infectious humans	1/10/day	[32]
η_2	Recovery rate of carrier humans	1/3/year	[14]
ϵ_1	Pathogens shedding rate into the water sources by infectious human	80 cells/mL/day	Assumed
ϵ_2	Pathogens shed rate into the water supply by carriers	70 cells/mL/day	Assumed
r	(Maximum) per capita growth rate of amebiasis pathogens	0.73/day	[33]
μ_b	Mortality rate of amebiasis pathogens, including phage degradation	0.83/day	[25]
ϕ	Wanning rate of diseased induced immunity	1/17/year	[34]
χ	Rate at which sanitation leads to death of *amebiasis* pathogens	$2\mu_b$/year	[25]
τ	Treatment rate for infectious individuals (I)	0.4/year	Assumed
f	Fraction of exposed individuals who progress to infectious class (I)	0.1	[15]
γ	Progression rate for infectious individuals to carriers ($I \to C$)	0.4/year	Assumed
θ	Progression rate for carriers to infectious individuals ($C \to I$)	0.6/year	Assumed

over time. These reservoirs can become contaminated with pathogens from various sources, such as human feces or intermediate hosts. An extra compartment, $B(t)$, is devised, representing the reservoir of amebiasis pathogens in the surroundings, as amebiasis is frequently contracted by consuming contaminated matter such as water or food [6]. Susceptible individuals are assumed to join the population at a steady rate Λ. Amebiasis infection can be transmitted through direct contact with carriers or infected individuals (at a rate of $\lambda_h(t)$) or by consuming pathogens from polluted freshwater reservoirs (at a rate of $\lambda_b(t)$). To represent the cumulative infection force, use $\lambda(t)$:

$$\lambda(t) = \lambda_h(t) + \lambda_b(t), \tag{1}$$

where

$$\lambda_h(t) = \alpha_1 I(t) + \alpha_2 C(t),$$
$$\lambda_b(t) = \alpha_3 B(t).$$

Likewise, the parameters; α_1 and α_2 are the transmission rates for infectious and carriers individuals, respectively, while, $\alpha_3 > 0$ is individuals' ingestion rate of amebiasis pathogens. The exposed population can join infectious or carrier classes. A proportion, f, of the exposed population proceeds to the contagious phase at a rate denoted by δ. In contrast, the remaining population undergoes an analogous transition to the carrier stage at the same rate. Attempts to eradicate amebiasis are made more difficult because carriers show no signs of the disease despite still being contagious. Some infected individuals recover naturally at the rate η_1 or through treatment at a rate τ, while others may progress to becoming carriers at a rate γ. This assumption is consistent with [10], who confirmed the presence of possible treatments for amebiasis. Based on studies by [27–29], it has been found that only a minority (one in every four) of asymptomatic individuals with *Entamoeba histolytica* infections progress to develop clinical symptoms. Thus, it is reasonable to assume that the carriers may regress to infectious class at the rate θ, while others may recover naturally at the rate η_2. Since amebiasis is known to be fatal [4], infectious individuals and carriers may die from amebiasis at rates of d_1 and d_2, respectively. Any individuals from each compartment may also experience natural death, modeled by a rate of μ. It is also acknowledged that amebiasis generates a temporary immunity that vanishes at a rate of ϕ over time. As a result, fully recovered patients may re-enter the susceptible population after losing their immunity.

Infected people discharge pathogens into the surroundings at two different rates, ϵ_1 and ϵ_2, depending on whether they are in state $I(t)$ or state $C(t)$. It is hypothesized that individuals from compartment I shed at the rate ϵ_1, notably higher than that of the carrier group (C), ϵ_2. It is important to remember that the C group play an essential role in the transmission dynamics of amebiasis, even though they shed few pathogens and remain symptom-free for extended periods [30]. Amebiasis pathogens multiply by birth and increase at the rate r and decay naturally at the rate μ_b or diminish through sanitation measures at the rate χ. In this scenario, r is assumed to be less than μ_b, so pathogen growth does not surpass mortality; this assumption is made to make our model realistic with epidemiological meaningful solutions. Detailed descriptions of the model's parameters are in Table 1. Fig. 1 presents the flow diagram for the dynamics of amebiasis.

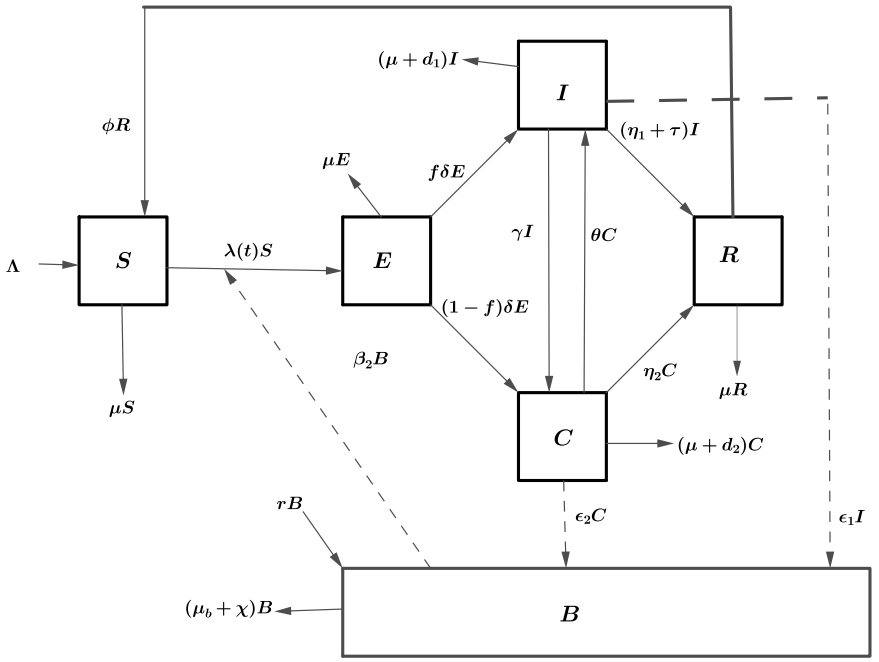

Fig. 1. A flow diagram for amebiasis transmission dynamics.

From the above descriptions, the following model is established and presented by a coupled system of differential equations:

$$\begin{aligned}
\frac{dS}{dt} &= \Lambda + \phi R - (\lambda(t) + \mu)S,\\
\frac{dE}{dt} &= \lambda(t)S - (\mu + \delta)E,\\
\frac{dI}{dt} &= f\delta E + \theta C - (\mu + d_1 + \eta_1 + \gamma + \tau)I,\\
\frac{dC}{dt} &= (1-f)\delta E + \gamma I - (\mu + d_2 + \eta_2 + \theta)C,\\
\frac{dR}{dt} &= (\eta_1 + \tau)I + \eta_2 C - (\mu + \phi)R,\\
\frac{dB}{dt} &= rB + \epsilon_1 I + \epsilon_2 C - (\mu_b + \chi)B.
\end{aligned} \tag{2}$$

The initial conditions for the model system (2) are $S(0) > 0, E(0) \geq 0, I(0) \geq 0, C(0) \geq 0, R(0) \geq 0, B(0) \geq 0$.

2.1. Boundedness of solutions

The human population, denoted by T_H, and the number of pathogens in the aquatic setting, denoted by T_B, are two distinct components of the model system (2) $T_H = \{(S(t), E(t), I(t), C(t), R(t)) \in \mathbb{R}^5_+ : S(t)+E(t)+I(t)+C(t)+R(t) = N(t)\}$ and $T_B = \{B(t) \in \mathbb{R}^1_+\}$ respectively.

From the model system (2), the differential inequality of the susceptible population is given by

$$\frac{dS}{dt} + \mu S \leq \Lambda + \phi R. \tag{3}$$

The differential inequality (3) can be solved to obtain

$$S(t) \leq \frac{\Lambda}{\mu} + e^{-\mu t}\int_0^t \phi R(x) e^{-\mu x} dx. \tag{4}$$

Applying the theorem of differential inequality by Birkhoff and Rota [35], we obtain

$$\lim_{t\to\infty} \sup S(t) \leq \frac{\Lambda}{\mu}.$$

Therefore, a susceptible population's state variable is less than or equal to the quotient of the recruitment rate and the natural death rate. We must also into account that $N = S + E + I + C + R$, reflects the total population. Differentiate N with respect to t i.e $\frac{dN}{dt}$, plug the equations of system (2) into the resulting expression gives

$$\frac{dN}{dt} = \Lambda - \mu N - d_1 I - d_2 C. \tag{5}$$

Solving the corresponding Eq. (5) with N^0 as the initial population yields the following results:

$$N(t) \leq \frac{\Lambda}{\mu} - (\frac{\Lambda}{\mu} - N^0)e^{-\mu t}, \tag{6}$$

therefore,

$$\lim_{t\to\infty} \sup N(t) \leq \frac{\Lambda}{\mu}$$

Since N is the total population, each state variable is less or equal to $\frac{\Lambda}{\mu}$. Using the equation for B from the system (2), We obtain a differential inequality:

$$\frac{dB}{dt} + (\mu_b + \chi - r)B = \epsilon_1 I + \epsilon_2 C \leq (\epsilon_1 + \epsilon_2)\frac{\Lambda}{\mu},$$

which simplifies to

$$\frac{dB}{dt} + (\mu_b + \chi - r)B \leq (\epsilon_1 + \epsilon_2)\frac{\Lambda}{\mu}. \tag{7}$$

The solution to Eq. (7) can be obtained by using integrating factors to get

$$B(t) = \frac{(\epsilon_1 + \epsilon_2)\Lambda}{\mu(\mu_b + \chi - r)} + B_0 e^{-(\mu_b+\chi-r)t},$$

where $B_0 = B(0)$, is an initial solution. Therefore,

$$\lim_{t\to\infty} \sup B(t) \leq \frac{(\epsilon_1 + \epsilon_2)\Lambda}{\mu(\mu_b + \chi - r)}.$$

Hence, the domain of biological significance of the system (2) is

$$T = \left[S, E, I, C, R, B \geq 0 : S + E + I + C + R \leq \frac{\Lambda}{\mu}, B \leq \frac{(\epsilon_1 + \epsilon_2)\Lambda}{\mu(\mu_b + \chi - r)}\right]. \tag{8}$$

Under the flow induced by the system (2), the domain T is positively invariant . Consequently, it is feasible to evaluate the model, within the field T, hence the system (2) has biological importance.

2.2. Existence of equilibrium solutions

Here, we will show whether or not the equilibrium exists. By making the right-hand side (2) equal to zero and then solving the obtained system, we may find the equilibrium points:

$$\begin{aligned}
0 &= \Lambda + \phi R^* - (\lambda^*(t) + \mu)S^*,\\
0 &= \lambda^*(t)S^* - (\mu + \delta)E^*,\\
0 &= f\delta E^* + \theta C^* - (\mu + d_1 + \eta_1 + \gamma + \tau)I^*,\\
0 &= (1 - f)\delta E^* + \gamma I^* - (\mu + d_2 + \eta_2 + \theta)C^*,\\
0 &= (\eta_1 + \tau)I^* + \eta_2 C^* - (\mu + \phi)R^*,\\
0 &= rB^* + \epsilon_1 I^* + \epsilon_2 C^* - (\mu_b + \chi)B^*.
\end{aligned} \tag{9}$$

where

$$\lambda^*(t) = \alpha_1 I^* + \alpha_2 C^* + \alpha_3 B^*. \tag{10}$$

To simplify the process of solving the system (9), let $w_0, w_2, w_3 > 0$ such that

$$\begin{aligned}
w_0 &= \mu + \delta,\\
w_1 &= \mu + d_1 + \eta_1 + \gamma + \tau,\\
w_2 &= \mu + d_2 + \eta_2 + \theta,\\
w_3 &= \mu_b + \chi - r.
\end{aligned} \tag{11}$$

Solving the system (9), we have

$$\begin{aligned}
E^* &= h_1 I^*,\\
C^* &= h_2 I^*,\\
R^* &= h_3 I^*,\\
S^* &= \frac{\Lambda}{\mu} + \left(\frac{\phi h_3}{\mu} - \frac{(\mu + \delta)h_1}{\mu}\right) I^*,\\
B^* &= \left(\frac{\epsilon_1 + \epsilon_2 h_2}{w_3}\right) I^*.
\end{aligned} \tag{12}$$

where

$$h_1 = \frac{w_1 w_2 - \theta\gamma}{f\delta w_2 + (1-f)\delta\theta},$$
$$h_2 = \frac{f\delta + (1-f)w_1\delta}{f\delta w_2 + (1-f)\delta\theta},$$
$$h_3 = \frac{\eta_1 + \tau + \eta_2 h_2}{f\delta w_2 + (1-f)\delta\theta}.$$

It can be noted that

$$\lambda^* = \alpha_1 I^* + \alpha_2 C^* + \alpha_3 B^* = h_4 I^*, \tag{13}$$

where

$$h_4 = \alpha_1 + \alpha_2 h_2 + \frac{\alpha_3\left(\epsilon_1 + \epsilon_2 h_2\right)}{w_3}.$$

Plug in λ^*, S^* and E^* in second Eq. (9) to get

$$h_4 I^*\left(\frac{\Lambda}{\mu} + \left(\frac{\phi h_3}{\mu} - \frac{(\mu+\delta)h_1}{\mu}\right) I^*\right) = (\mu+\delta)h_1 I^*. \tag{14}$$

Solving (14) gives:

$$\begin{aligned} I^* &= 0, \\ I^* &= \frac{\Lambda}{\mu+\delta} + \frac{\phi h_3}{\mu+\delta} - \frac{1}{h_4}, \end{aligned} \tag{15}$$

$I^* = 0$ corresponds to the existence of disease-free whereas $I^* = \frac{\Lambda}{\mu+\delta} + \frac{\phi h_3}{\mu+\delta} - \frac{1}{h_4}$ corresponds to the existence of the endemic equilibrium point.

Disease Free Equilibrium Point

Disease-free equilibrium occurs when no new infections occur, preferably when $I^* = 0$, plug in this condition into Eq. (12) to obtain $E^* = C^* = R^* = B^* = 0$ and $S^* = \frac{\Lambda}{\mu}$. Hence, the disease-free equilibrium is given by

$$E_0 = (S^0, E^0, I^0, C^0, R^0, B^0) = \left(\frac{\Lambda}{\mu}, 0, 0, 0, 0, 0\right). \tag{16}$$

Endemic Equilibrium Point

The endemic equilibrium point occurs when the disease stabilizes in the community. This is a nontrivial equilibrium point of the model system (9): $S^*, E^*, I^*, C^*, R^*, B^* > 0$. The endemic equilibrium point for this scenario can be established by substituting the expression for I^* from Eq. (15) into Eq. (12).

2.3. Reproduction number and stability analysis of steady states

The two reproduction numbers most discussed in epidemiological studies are the basic reproduction number denoted by R_0 and the effective reproduction number R_e or R_t [36]. R_0 embodies the hypothetical transmission potential of a disease in a completely susceptible population with no interventions, whereas R_e reflects the actual transmission potential at a particular instant, considering immunity and intervention strategies. R_0 is a constant, while R_e can vary as outbreak conditions change. R_0 is a useful concept for comprehending the inherent contagiousness of a disease, whereas R_e aids in assessing the effect of control measures on disease transmission. Since our model has captured some control parameters as our goal is to investigate their impacts, it is, therefore, important to derive the effective number rather than the basic reproduction number.

In the context of disease control, R_e is a critical metric because it helps public health officials to understand how easily a disease can spread and to design effective strategies to control or prevent its transmission. If the value $R_e < 1$, the disease is unlikely to spread widely in a population. Therefore, it may be possible to control or eliminate the disease through sanitation, education campaigns, treatment, vaccination, contact tracing, quarantine, etc. However, if $R_e > 1$, it suggests the disease could spread fast, reaching epidemics or pandemic proportions. By understanding the R_e value of a disease, public health officials can design targeted interventions to reduce the number of new infections and bring $R_e < 1$. Ultimately, disease control aims to reduce R_e to a level where the disease is no longer a significant public health threat.

The magnitude of R_e also allows us to evaluate the stability of the equilibria and, hence, the presence or absence of the disease from the community. Each infected person will spread the disease to less than one individual if $R_e < 1$; therefore, the disease will die out. Also, each infected person can spread the disease to more than one other person when $R_e > 1$, leading to an epidemic. A

large value of R_e number might suggest an alarming disease outbreak. In this study, the expression for R_e is determined following the next-generation operator method [37,38]. The procedure includes determining the spectral radius of the matrix

$$FV^{-1} = \left[\frac{\partial \mathcal{F}_i\,(E_0)}{\partial x_j}\right]\left[\frac{\partial \mathcal{V}_i\,(E_0)}{\partial x_j}\right]^{-1}, \tag{17}$$

where $\mathcal{F}_i$ represents the rate at which new infections emerge in compartment i, $\mathcal{V}_i$ is the transfer of infections from compartment i to another and E_0 is the disease-free equilibrium. The equations involving the infectious classes of E, I, C, and B are rewritten based on the system in (2). Consequently, the system

$$\begin{aligned}
\frac{dE}{dt} &= \lambda(t)S - w_0E,\\
\frac{dI}{dt} &= \delta E - w_1I,\\
\frac{dC}{dt} &= \gamma I - w_2C,\\
\frac{dB}{dt} &= \epsilon_1 I + \epsilon_2 C - w_3B.
\end{aligned} \tag{18}$$

where w_0, w_1, w_2, w_3 are defined in Eq. (11). From Eq. (18) one can extract:

$$\mathcal{F}_i = \begin{bmatrix} \alpha_3 BS + \alpha_1 IS + \alpha_2 CS \\ 0 \\ 0 \\ 0 \end{bmatrix}, \tag{19}$$

$$\mathcal{V}_i = \begin{bmatrix} w_0E \\ w_1I - \delta E \\ w_2C - \gamma I \\ (\mu_b + \chi - r)B - \epsilon_1 I - \epsilon_2 C \end{bmatrix}. \tag{20}$$

By determining the partial derivative of $\mathcal{F}_i$ and $\mathcal{V}_i$ with respect to E, I, C and B at E_0, we obtain

$$F = \begin{bmatrix} 0 & \alpha_1 S^0 & \alpha_2 S^0 & \alpha_3 S^0 \\ 0 & 0 & 0 & 0 \\ 0 & 0 & 0 & 0 \\ 0 & 0 & 0 & 0 \end{bmatrix}, \tag{21}$$

$$V = \begin{bmatrix} w_0 & 0 & 0 & 0 \\ -f\delta & w_1 & -\theta & 0 \\ f-1 & -\gamma & w_2 & 0 \\ 0 & -\epsilon_1 & -\epsilon_2 & w_3 \end{bmatrix}. \tag{22}$$

Therefore, the effective reproduction number (R_e) is

$$R_e = \rho(FV^{-1}) = R_1 + R_2 + R_3, \tag{23}$$

where

$$\begin{aligned}
R_1 &= \frac{\left(f\delta w_2 + (1-f)\theta\right)\alpha_1 S^0}{\left(w_2w_1 - \gamma\theta\right)w_0},\\
R_2 &= \frac{\left(w_1(1-f) + \gamma f\delta\right)\alpha_2 S^0}{\left(w_2w_1 - \gamma\theta\right)w_0},\\
R_3 &= \frac{\left(\epsilon_1 f\delta w_2 + \epsilon_2\gamma f\delta + (1-f)\left(\epsilon_1\theta + \epsilon_2 w_1\right)\right)\alpha_3 S^0}{\left(w_2w_1 - \gamma\theta\right)w_0w_3},
\end{aligned}$$

while terms w_0, w_1, w_2 and w_3 have been defined in (11), whereas, S^0 is defined in Eq. (16). Additionally, R_1, R_2, and R_3 denotes the partial reproduction number generated by I-to-S, C-to-S, and B-to-S transmission, respectively.

2.4. Local stability of disease-free equilibrium

In this part we prove for the local stability of disease-free equilibrium determined in (16). We begin by stating the theorem below:

Theorem 1. *The DFE of the model system (2) is locally asymptotically stable if $R_e < 1$ and unstable if $R_e > 1$.*

Proof. The Jacobian Matrix J is obtained by partially differentiating the system (2) with respect to (S, E, I, C, R, B) at the disease-free equilibrium.

$$J(E_0) = \begin{bmatrix} -\mu & 0 & -\alpha_1 S_0 & -\alpha_2 S_0 & \phi & -\alpha_3 S_0 \\ 0 & -w_0 & \alpha_1 S_0 & \alpha_2 S_0 & 0 & \alpha_3 S_0 \\ 0 & \delta & -w_1 & 0 & 0 & 0 \\ 0 & 0 & \gamma & -w_2 & 0 & 0 \\ 0 & 0 & \eta_1 + \tau & \eta_2 & -w_3 & 0 \\ 0 & 0 & \epsilon_1 & \epsilon_2 & 0 & -w_4 \end{bmatrix}. \tag{24}$$

where w_0, w_1 and w_2 have been defined in Eq. (11). The matrix (24) has two trivial negative eigenvalues $\lambda = -\mu$ and $\lambda = -w_3 = -(\mu_b + \chi - r)$. If we set $H_{11} = w_0, H_{12} = \alpha_1 S_0, H_{13} = \alpha_2 S_0, H_{14} = S_0\alpha_3, H_{21} = \delta, H_{22} = w_1, H_{32} = \gamma$, $H_{33} = w_2, H_{42} = \epsilon_1, H_{43} = \epsilon_2, H_{44} = \mu_b + \chi - r$, then the remaining 4×4 sub-matrix is given as:

$$J_1(E_0) = \begin{bmatrix} -H_{11} & H_{12} & H_{13} & H_{14} \\ H_{21} & -H_{22} & 0 & 0 \\ 0 & H_{32} & -H_{33} & 0 \\ 0 & H_{42} & H_{43} & -H_{44} \end{bmatrix}. \tag{25}$$

The rest of the eigenvalues are the roots of the polynomial: $|J_1(E_0) - \lambda| = 0$, which is given by

$$\lambda^4 + c_3\lambda^3 + c_2\lambda^2 + c_1\lambda + c_0 = 0, \tag{26}$$

where the constants are such that

$$\begin{aligned} c_3 =& H_{11} + H_{22} + H_{33} + H_{44}, \\ c_2 =& \left(H_{44}H_{33} + H_{44}H_{22} + H_{44}H_{11} + H_{33}H_{22} + H_{33}H_{11} + H_{22}H_{11}(1 - R_d)\right), \\ c_1 =& H_{11}H_{22}H_{44}\left(1 - \left(R_a + R_d\right)\right) + H_{11}H_{22}H_{33}\left(1 - \left(R_c + R_d\right)\right) \\ &+ H_{22}H_{33}H_{44} + H_{11}H_{33}H_{44}, \\ c_0 =& H_{44}H_{33}H_{22}H_{11}\left(1 - R_e\right). \end{aligned}$$

Moreover, R_e can be split into parts

$$R_e = R_a + R_b + R_c + R_d, \tag{27}$$

where

$$\begin{aligned} R_a &= \frac{H_{43}H_{32}H_{21}H_{14}}{H_{44}H_{33}H_{22}H_{11}}, \\ R_b &= \frac{H_{42}H_{21}H_{14}H_{33}}{H_{44}H_{33}H_{22}H_{11}}, \\ R_c &= \frac{H_{44}H_{32}H_{21}H_{13}}{H_{44}H_{33}H_{22}H_{11}}, \\ R_d &= \frac{H_{44}H_{33}H_{21}H_{12}}{H_{44}H_{33}H_{22}H_{11}}. \end{aligned}$$

To ensure that all roots of Eq. (26) have negative real parts, the Routh–Hurwitz stability criterion (for further details refer [39,40]) requires that

$$c_3 > 0, c_2 > 0, c_1 > 0, c_0 > 0, \tag{28}$$

and

$$\begin{aligned} D_1 &= c_3 > 0, \\ D_2 &= \begin{vmatrix} c_3 & 1 \\ c_1 & c_2 \end{vmatrix} = c_3c_2 - c_1 > 0, \\ D_3 &= \begin{vmatrix} c_3 & 1 & 0 \\ c_1 & c_2 & c_3 \\ 0 & c_0 & c_1 \end{vmatrix} = c_1c_2c_3 - c_1^2 - c_0c_3^2 > 0, \\ D_4 &= \begin{vmatrix} c_3 & 1 & 0 & 0 \\ c_1 & c_2 & c_3 & 1 \\ 0 & c_0 & c_1 & c_2 \\ 0 & 0 & 0 & c_0 \end{vmatrix} = c_0\left(c_1c_2c_3 - c_1^2 - c_0c_3^2\right) > 0. \end{aligned} \tag{29}$$

It is obvious that $D_1 = c_3 > 0$. In addition, if $R_e < 1$, it implies that $R_a, R_b, R_c, R_d < 1$ and hence $c_0, c_1, c_2 > 0$. Also, D_2 can be shown to be positive as follows:

$$\begin{aligned} D_2 = {} & (H_{11} + H_{22} + H_{33} + H_{44})(H_{11}H_{33} + H_{11}H_{44} + H_{22}H_{33} + H_{22}H_{44} + H_{33}H_{44} + H_{11}H_{22}(1 - R_d)) \\ & - H_{11}H_{33}H_{44} - H_{22}H_{33}H_{44} - H_{11}H_{22}H_{44}(1 - R_a - R_d) - H_{11}H_{22}H_{33}(1 - R_c - R_d), \end{aligned}$$

The only remaining condition to show is

$$D_3 = c_1(c_2c_3 - c_1) - c_0c_3^2 > 0. \tag{30}$$

To prove the inequality (30) , it is sufficient to establish the following two inequalities:

$$c_1c_2c_3 > 2c_1^2, \tag{31}$$

$$c_1c_2c_3 > 2c_0c_3^2. \tag{32}$$

To show (31), we write $c_2c_3 - 2c_1$ into the sum of the following parts:

$$\begin{aligned} c_2c_3 - 2c_1 = {} & H_{11}H_{33}^2 + H_{11}^2H_{33} + H_{11}H_{44}^2 + H_{22}H_{33}^2 + H_{11}^2H44 \\ & + H_{22}^2H_{33} + H_{22}H44^2 + H_{22}^2H44 + H_{33}H44^2 + H_{33}^2H44 + H_{11}H_{22}H_{33} + H_{11}H_{22}H_{44} \\ & + H_{11}H_{33}H_{44} + H_{22}H_{33}H_{44} + H_{11}H_{22}^2(1 - R_d) + H_{11}^2H_{22}(1 - R_d) \\ & + 2H_{11}H_{22}H_{44}R_a + 2H_{11}H_{22}H_{33}R_c + H_{11}H_{22}H_{33}R_d + H_{11}H_{22}H_{44}R_d. \end{aligned}$$

Similarly, to show (32), we write $c_1c_2 - 2c_0c_3$ into the sum of parts as follows:

$$\begin{aligned} c_1c_2 - 2c_0c_3 = {} & H_{11}H_{33}^2H_{44}^2 + H_{11}^2H_{33}H_{44}^2 + H_{11}^2H_{33}^2H_{44} + H_{22}H_{33}^2H_{44}^2 + H_{22}^2H_{33}H_{44}^2 + H_{22}^2H_{33}^2H_{44} \\ & + H_{11}H_{22}^2H_{44}^2(1 - R_a - R_d) + H_{11}^2H_{22}H_{44}^2(1 - R_a - R_d) \\ & + H_{11}^2H_{22}^2H_{44}(1 - R_a - 2R_d + R_aR_d + R_d^2) + H_{11}H_{22}^2H_{33}^2(1 - R_c) \\ & + H_{11}^2H_{22}H_{33}^2(1 - R_c - R_d) + H_{11}^2H_{22}^2H_{33}(1 - R_c - 2R_d + R_d^2 + R_cR_d) \\ & + H_{11}H_{22}^2H_{33}^2(1 - R_c - R_d) + H_{11}H_{22}H_{33}H_{44}^2 + H_{11}H_{22}H_{33}^2H_{44} + H_{11}H_{22}H_{33}H_{44}^2R_a \\ & + 2H_{11}H_{22}H_{33}^2H_{44}R_a + H_{11}H_{22}^2H_{33}H_{44}R_a + H_{11}^2H_{22}H_{33}H_{44}R_a \\ & + 2H_{11}H_{22}H_{33}H_{44}^2R_b + 2H_{11}H_{22}H_{33}^2H_{44}R_b + 2H_{11}H_{22}^2H_{33}H_{44}R_b \\ & + 2H_{11}^2H_{22}H_{33}H_{44}R_b + 2H_{11}H_{22}H_{33}H_{44}^2R_c + H_{11}H_{22}H_{33}^2H_{44}R_c + H_{11}H_{22}^2H_{33}H_{44}R_c \\ & + H_{11}^2H_{22}H_{33}H_{44}R_c + H_{11}H_{22}H_{33}H_{44}^2R_d + H_{11}H_{22}H_{33}^2H_{44}R_d \\ & + H_{11}H_{22}^2H_{33}H_{44}(1 - R_d) + H_{11}^2H_{22}H_{33}H_{44}(1 - R_d) + H_{11}^2H_{22}^2H_{44}R_aR_d. \end{aligned}$$

It can be noted that if $R_e < 1$, then each $R_a, R_b, R_c, R_d < 1$ and therefore $c_1c_2 - 2c_0c_3 > 0$ and $c_2c_3 - 2c_1 > 0$. With these results, it can be concluded that Eqs. (31) and (32) hold, and so does the condition (30). Moreover, the proof for condition D_4 can be established from $D_4 = c_0D_3$. Fortunately, we have already proved that $D_3 > 0$. Therefore, it is clear that $D_4 = c_0D_3 > 0$. Thus, all conditions of Routh–Hurwitz for this case (Eqs. (28) and (29)) are satisfied, then the disease-free equilibrium E_0 is locally asymptotically stable whenever $R_e < 1$. □

2.5. Global stability of disease-free equilibrium point

The following result is presented based on the global stability of the disease-free equilibrium.

Theorem 2. *If $R_e < 1$, the disease-free equilibrium point is globally asymptotically stable and unstable if $R_e > 1$.*

Proof. Using the comparison theorem [41], the rate of change of the variables representing the infected components of the model system (2) can be re-written as,

$$\begin{pmatrix} \frac{dE}{dt} \\ \frac{dI}{dt} \\ \frac{dC}{dt} \\ \frac{dB}{dt} \end{pmatrix} = (F - V) \begin{pmatrix} E \\ I \\ C \\ B \end{pmatrix} - \begin{pmatrix} 0 & \alpha_1S^0 & \alpha_2S^0 & \alpha_3S^0 \\ 0 & 0 & 0 & 0 \\ 0 & 0 & 0 & 0 \\ 0 & 0 & 0 & 0 \end{pmatrix} \begin{pmatrix} E \\ I \\ C \\ B \end{pmatrix}, \tag{33}$$

implying that

$$\begin{pmatrix} \frac{dE}{dt} \\ \frac{dI}{dt} \\ \frac{dC}{dt} \\ \frac{dB}{dt} \end{pmatrix} \leq (F - V) \begin{pmatrix} E \\ I \\ C \\ B \end{pmatrix}, \tag{34}$$

Table 2
Parameters and their Sensitivity Indices.

Parameter	Sensitivity index	Parameter	Sensitivity index
Λ	+1.0000	d_2	−0.0364
α_1	+0.0134	η_1	−0.0416
α_2	+0.0068	η_2	−0.0364
α_3	+0.9799	ϵ_1	+0.5855
γ	−0.0192	ϵ_2	+0.3943
δ	−0.2883	r	+0.1633
μ	−1.9958	τ	−0.2082
μ_b	−0.6532	θ	+0.19395
χ	−0.4899	f	−0.0985
d_1	−0.1561		

with F and V being Jacobian matrices see (21) and (22). Following the stability results of Theorem 1, we know that the eigenvalues of the matrix $(F-V)$ have negative real components, then system (2) is stable whenever $R_e < 1$. So $(S, E, I, C, B, R) \to (S^0, 0, 0, 0, 0, 0)$ and $S \to S_0$ as $t \to \infty$. By the comparison theorem (see [41] for details) $(S, E, I, C, B, R) \to E_0$ as $t \to \infty$. Therefore, E_0 is globally asymptotically stable whenever $R_e < 1$. □

The epidemiological significance of Theorem 2 is that it provides important insights into disease control and prevention strategies. Public health officials can determine whether or not the disease is likely to become endemic in a population by estimating the basic reproduction number of a disease. Suppose the basic reproduction number is less than one; in that case, the disease is unlikely to become established in the population, and public health officials may focus their efforts on preventing the introduction of the disease into the population or on quickly identifying and treating individuals who become infected.

3. Sensitivity analysis

In a nutshell, sensitivity analysis looks into how changing the model's inputs affects the results. This analysis contributes to the rise of confidence regarding the model by evaluating uncertainties connected to its parameters, which the analysis can alter. This method is frequently used to evaluate the model's sensitivity to changes in input parameters because of its usefulness in providing rough estimates of the effects of such changes. That is why it is useful for prioritizing intervention efforts by showing which factors impact the model most.

Here, we will explore the two main types of sensitivity analysis approaches: local and global, and their respective implications.

3.1. Local sensitivity analysis

Unlike global sensitivity analysis, which considers the variation introduced by all input parameters, local sensitivity analysis evaluates the effect of each parameter on the model at distinct points within the parameter space.

Using the effective reproduction number R_e established by Eq. (23), we will determine the model's local sensitivity (2). An analytical expression for the sensitivity index will be derived using the normalized forward sensitivity index as defined by [42].

$$\Pi_{\Lambda}^{R_e} = \frac{\partial R_e}{\partial \Lambda} \times \frac{\Lambda}{R_e} = +1 \tag{35}$$

$$\Pi_{\mu}^{R_e} = \frac{\partial R_e}{\partial \mu} \times \frac{\mu}{R_e} = -1.9958 \tag{36}$$

The rest of the sensitivity indices for all parameters used in Eq. (23) can be computed similarly. Table 2 shows the sensitivity indices of R_e for all parameters.

From Table 2, we can obtain $\Pi_{\mu}^{R_e} = -1.9958$, this means that an increase in μ will cause a decrease in R_e. Similarly, a decrease in μ will cause an increase in R_e, as they are inversely proportional. We can also note that $d_1, d_2, \eta_1, \eta_2, \mu_b, \gamma, \tau$ and χ are all negative hence these parameters are inversely proportional to R_e. This means that if any of these factors is increased (decreased), R_e will decrease (increase).

Nonetheless, it can be noted that $\Pi_{\Lambda}^{R_e} = +1$ implies any rise in Λ will result in an equal rise in R_e. Conversely, if you reduce Λ, R_e will also go down because the two quantities are inversely proportional. We can also note that the indices for $\alpha_1, \alpha_2, \alpha_3, \epsilon_1, \epsilon_2, \theta$ or $r > 0$ hence these parameters are directly proportional to R_e. Since this is the case, changing any of these variables will affect R_e. The following is a ranking of these parameters from largest to lowest by order of magnitude: $\mu, \Lambda, \alpha_3, \mu_b, \epsilon_1, \delta, d_1, \chi, \gamma, \eta_1, \epsilon_2, d_2, \alpha_1, \eta_2$ and α_2. When the parameters associated with control measures (χ and τ) are increased, the effective reproduction number R_e decreases. That means these parameters can be used as useful control interventions. Therefore, the spread of the disease can be stopped with the right mix of sanitation and therapy. To the contrary, the findings suggest that exposure to contaminated surroundings (α_3) may be more influential than human-to-human contacts (α_1 or α_2) in accelerating disease replication. The finding aligns with the research of other scholars, including Haque et al. in 2003 [43]. There are substantial implications for the public and policymakers alike from these findings. Access to basic sanitary services, such as potable water, toilets, and waste disposal, must be universally guaranteed. The prevalence of various diseases, such as diarrhea-related illnesses, can be lowered dramatically with the help of such efforts.

Table 3
Parameter value ranges of model (2) used as input for the LHS method.

Parameter	Range	Parameter	Range
Λ	[75, 125]	d_2	[0.45, 0.75]
α_1	[0.03, 0.05]	η_1	[0.03, 0.05]
α_2	[0.225, 0.375]	η_2	[0.0375, 0.0625]
α_3	[0.0375, 0.0625]	ϵ_1	[22.5, 37.5]
γ	[0.15, 0.25]	ϵ_2	[15, 25]
δ	[0.05355, 0.08925]	r	[0.15, 0.25]
μ	[0.12525, 0.20875]	τ	[0.225, 0.375]
μ_b	[0.225, 0.375]	θ	[0.3, 0.5]
χ	[0.075, 0.125]	f	[0.15, 0.25]
d_1	[0.1125, 0.1875]		

Table 4
Parameters and their PRCC values.

Parameter	PRCCs	Parameter	PRCCs
Λ	+0.3325	d_2	−0.1354
α_1	+0.002554	η_1	−0.01102
α_2	+0.02667	η_2	−0.02208
α_3	+0.3422	ϵ_1	+0.1522
γ	+0.03469	ϵ_2	+0.04421
δ	+0.1884	r	+0.2805
μ	−0.5893	τ	−0.09592
μ_b	−0.4807	θ	+0.05855
χ	−0.1486	f	+0.04498
d_1	−0.01683		

3.2. Global sensitivity analysis

Global sensitivity analysis is the practice of allocating the uncertainty in outcomes to the uncertainty associated with each data point across their whole spectrum of relevance. The global sensitivity analysis occurs when all inputs are changed simultaneously, and the sensitivity is evaluated across the whole range of each input a component as stated by [44]. We utilize a global sensitivity analysis to investigate at the model's vulnerability to changes in a wider range of parameters. Parameter means are shown in Table 1, and the range values of these parameters are given in Table 3.

Since the effective reproductive number is parameter-dependent, we must emphasize that adjusting any of the model's parameters results in a degree of uncertainty in our predictions. The partial rank correlation coefficients (PRCCs) between the effective reproduction number R_e and each parameter in the model (2) are shown in Fig. 2, and were computed using the method described by [45]. Since the data regarding the distribution function was lacking, we made the choice for a uniform distribution for all parameters instead. Using Latin Hypercube Sampling (LHS), we generated a thousand simulation iterations with different input parameters. Partial Rank Correlation Coefficients were then calculated between R_e and each model parameter in (2). The PRCC's findings are as presented in Table 4. It is essential to note that the parameters with the highest PRCC values significantly impact the model 1. Table 4 shows that the parameter μ has the highest influence on the reproduction number R_e, followed in decreasing order by the parameters $\mu_b, \epsilon_1, \Lambda, r, \delta, \alpha_3, \chi, d_2$ and τ. The rest parameters: $\theta, f, \eta_2, \gamma, \alpha_2, \eta_2, d_1, \eta_1$ and α_1 have less effect on R_e.

It can be observed that parameters such as $\mu, \mu_b, \chi, d_2, \tau, \eta_2, d_2$ and η_1 assist us in significantly reducing the number of infections. As a result, the sensitivity analysis consistently supports our contention that the most effective way to combat infection is to increase sanitation and treatment strategies. It is worth noting that the order of the most essential parameters for R_e in the local sensitivity analysis differs from that in the global sensitivity analysis. Thus, the global results are considered more robust than the local ones.

4. Optimal control problem and analysis

The previous model (2) is extended in the present section by including three time-dependent controls representing awareness programs, treatment, and sanitation. In this case, the control interventions are regarded as time-dependent variables rather than constant parameters, as presented previously, thus allowing optimal disease control. An optimal control problem is formulated from the model presented in Eq. (2), with the parameters provided in Tables 1.

The success of awareness programs has been widely documented by researchers (e.g., [23,46]) in addressing various diseases. Likewise, in the present work, an awareness program is considered one of the essential measures in controlling amebiasis. Thus, the awareness program is modeled by a function $u_1(t)$. Next, it is assumed that treating patients who suffer from amebiasis helps

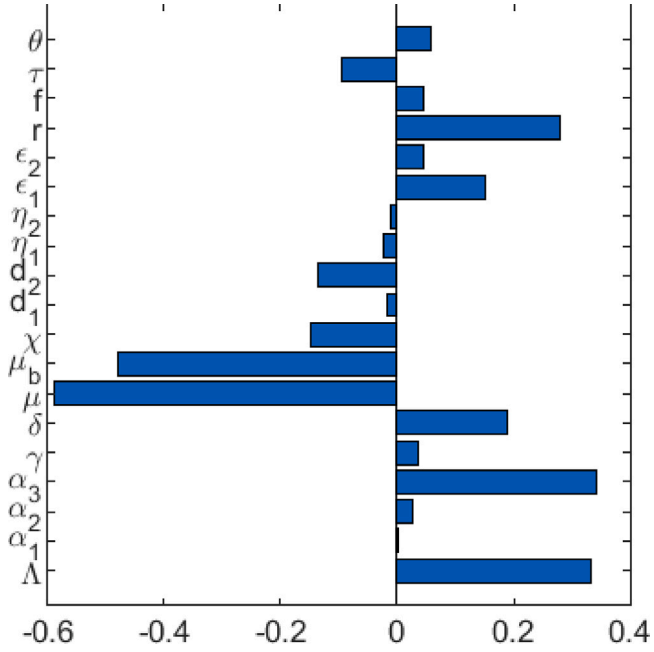

Fig. 2. Tornado plots of PRCC of parameters that influence model (2) generated using parameter values in Table 3. Parameters with $PRCC > 0$ and $PRCC < 0$ increase and decrease value of R_c, respectively.

minimize the spread of the disease. Untreated patients might develop severe associated symptoms. Therefore, infectious individuals are treated at the rate $u_2(t)$, and upon treatment, they may recover and join recovery class R. Furthermore, sanitation (including water treatment and safe disposal of waste) is assumed to reduce environmental pathogen concentrations (see also [47]). Therefore, sanitation effort is modeled by a control variable $u_3(t)$. This control is expected to reduce the concentration of pathogens in the environment (including water sources and foods). Based on the above descriptions, we obtain the following optimal control model:

$$\begin{aligned}
\frac{dS}{dt} &= \Lambda + \phi R - ((1-u_1)(\alpha_1 I + \alpha_2 C + \alpha_3 B) + \mu)S,\\
\frac{dE}{dt} &= (1-u_1)(\alpha_1 I + \alpha_2 C + \alpha_3 B)S - (\mu+\delta)E,\\
\frac{dI}{dt} &= f\delta E + \theta C - (\mu + d_1 + \eta_1 + \gamma + (1+u_2)\tau)I,\\
\frac{dC}{dt} &= (1-f)\delta E + \gamma I - (\mu + d_2 + \theta + \eta_2(1+u_2))C,\\
\frac{dR}{dt} &= (\eta_1 + (1+u_2)\tau)I + \eta_2(1+u_2)C - (\mu+\phi)R,\\
\frac{dB}{dt} &= rB + \epsilon_1(1-u_1)I + \epsilon_2(1-u_1)C - (\mu_b + \chi(1+u_3))B,
\end{aligned} \tag{37}$$

with initial conditions $S(0) > 0; E(0) \geq 0; I(0) \geq 0; C(0) \geq 0; R(0) \geq 0; B(0) \geq 0$. Setting the controls $u_1 = u_2 = u_3 = 0$, one can obtain a model with constant controls, which was studied in (2), where its stability analysis was well presented.

4.1. Optimal control analysis

It is necessary to modify these control measures to minimize the number of infectious individuals, carriers, and amebiasis pathogens and the costs of administering these control strategies. Consideration must be given to the optimal control problem with the objective functional of the form

$$J = \min_u \int_0^{t_f} \left(A_1 I + A_2 C + A_3 B + \sum_{i=1}^{3} \frac{K_i}{2} u_i^2 \right) dt, \tag{38}$$

where t_f is the final time, and $A_j, j = 1,2,3$ are the weight constants associated with the number of infectious humans, carriers humans, and pathogens concentration, whereas $K_i, i = 1,2,3$ are the i^{th} weights of control relative to its cost implications. The quadratic terms $\frac{K_1}{2}u_1^2$, $\frac{K_2}{2}u_2^2$, and $\frac{K_3}{2}u_3^2$ represent the costs of control efforts on awareness programs, treatment, and sanitation

respectively. [48,49] ague that quadratic objective are used many times since the cost implementing a control would be nonlinear, so a simple nonlinear case should be taken. The costs can include funds needed for control implementation as well as the negative financial impact on the environment.

Some researchers used the squares of the control variables to infer the seriousness of medication's adverse effects. Excessive amounts of medications such as interleukin are harmful to the body of humans, which is why the functional has quadratic terms [50,51]. Besides, Gumel et al. 2006 [52] justify the use of a simple quadratic on controls in objective functional to avoid "bang–bang" or "singular" optimal control cases encountered when the objective functional is linear, which can be challenging to handle. Bang–bang means that the optimal control only takes on values at the upper and lower bounds of the control set, and finding the times at the switching from lower bound to upper bound (or vice versa) occurs is more complicated than the quadratic case treated. Generally, quadratic objective functional is commonly used in optimal control problems because of its ability to trade-off between performance and control effort and its convexity, which allows for efficient numerical optimization to get a globally optimal control strategy.

Focus should be placed on minimizing the value of the objective functional J. Therefore, the current task is to identify the optimal control strategy under the criterion:

$$J(u^*) = \min J(u|u \in U),$$

where $U = \{(u_1, u_2, u_3)|u_i$ is Lebesgue measurable with $0 \leq U \leq 1$ for $t \in [0, t_f], i = 1, 2, 3\}$ is the set of admissible controls. The optimal control problem entails determining the existence and uniqueness of optimal controls and characterizing them.

4.2. The existence of the optimal controls

The current part explores the existence of optimal control framework (37) and Eq. (38) using a technique as presented in [53]. The following theorem is presented to aid the protocol of establishing existence stated.

Theorem 3. *Consider an objective functional $J(u)$, subject to the state Eq. (2) with non-negative initial solutions, then there exists an optimal control u^* and corresponding (S, E, I, C, R, B), that minimizes $J(u)$ over U.*

Proof. To employ the existing results by [54] [Theorem 4.1. page 68 - 70], first verify whether the following properties hold:

1. A set of controls with associated state variables is not empty.
2. Convexity and closure property holds in the set of controls.
3. Every right-hand side of the state system has the following properties: continuous, bounded above by the total of control and state and may be expressed in terms of u with time and state-varying coefficients.
4. The objective functional has a convex integrand $p(f, u)$.
5. An objective functional's integrand must meet the following conditions:
   $p \geq q_1 \left(|u_1|^2 + |u_2|^2 + |u_3|^2\right)^{\frac{\beta^*}{2}} - q_2$ for some constants $q_1, q_2 > 0$, and $\beta^* \geq 1$.

The study conducted by [53] (Theorem 9.2.1, p. 182) offers proof to support the existence of the state system, hence confirming the realization of the first property. Based on the notion of a convex set, it could be concluded that the control set U holds the properties of convexity and closure. As a result, the second property is likewise true. Considering a linear state system with state solutions in u_i, it is easily noticed that the resulting solutions are bounded. Therefore, it concludes that the right-hand side of the system is also bounded and may be represented by a linear function with bounds.

Finally, there are $q_1, q_2 \geq 0$ and $\beta^* \geq 1$ satisfying $A_1 I + A_2 C + A_3 B + K_1 u_1^2(t) + K_2 u_2^2(t) + K_3 u_3^2(t) \geq q_1 \left(|u_1|^2 + |u_2|^2 + |u_3|^2\right)^{\frac{\beta^*}{2}} - q_2$, since the state variables are bounded. Hence, the existence of optimal control follows from the existence results by [54]. One can also get more insights into the above proof by referring to the work by [20]. □

4.3. Characterization of the optimal controls

Pontryagin's Maximum Principle [55] is used for demonstrating the optimal controls. The optimal control problem is converted into a point-wise Hamiltonian (H) minimization problem about u. The state variables are symbolized by x, the controls by U, the adjoint variables by L, and the differential of the i^{th} state variable, denoted by f. Our problem is, therefore, the inner product of the right-hand sides of the state equations and adjoint variables $(L_1, L_2, L_3, L_4, L_5, L_6)$ and the integrand of the objective functional. The Hamiltonian can be expressed in its simplest form as

$$H = A_1 I + A_2 C + A_3 B + \sum_{i=1}^{3} \frac{K_i}{2} u_i^2 + L f(t, x(t), u_i(t)). \tag{39}$$

In the expanded form, the Hamiltonian is:

$$\begin{aligned} H = {} & A_1 I + A_2 C + A_3 B + \frac{K_1}{2}u_1^2 + \frac{K_2}{2}u_2^2 + \frac{K_3}{2}u_3^2 \\ & + L_1\left(\Lambda + \phi R - ((1-u_1)(\alpha_1 I + \alpha_2 C + \alpha_3 B) + \mu)S\right) \\ & + L_2\left((1-u_1)(\alpha_1 I + \alpha_2 C + \alpha_3 B)S - (\mu+\delta)E\right) \\ & + L_3\left(f\delta E + \theta C - (\mu + d_1 + \eta_1 + \gamma + (1+u_2)\tau I)\right) \\ & + L_4\left((1-f)\delta E + \gamma I - (\mu + d_2 + \theta + \eta_2(1+u_2))C\right) \\ & + L_5\left((\eta_1 + (1+u_2)\tau)I + \eta_2(1+u_2)C - (\mu+\phi)R\right) \\ & + L_6\left(rB + \epsilon_1(1-u_1)I + \epsilon_2(1-u_1)C - (\mu_b + \chi(1+u_3))B\right). \end{aligned} \tag{40}$$

Theorem 4. *Given u_i^* is the set of optimal control, and x^* the corresponding set of solutions of the state system (2) that minimizes J over Ω; then there exists adjoint variables L such that*

$$\frac{dL}{dt} = -\frac{\partial H}{\partial x}, \text{ adjoint conditions and} \tag{41}$$

$$L(t_f) = 0, \text{ transversality conditions. Furthermore,} \tag{42}$$

$$\frac{\partial H}{\partial u} = 0, \text{at } u^*, \text{optimality conditions.} \tag{43}$$

Proof. Take the partial derivative of the Hamiltonian H with respect to the state variables to get the adjoint system. That is to say

$$\begin{aligned} \frac{dL_1}{dt} =& L_1\left(\left(1-u_1\right)\left(\alpha_1 I + \alpha_2 C + \alpha_3 B\right) + \mu\right) - L_2\left(1-u_1\right)\left(\alpha_1 I + \alpha_2 C + \alpha_3 B\right), \\ \frac{dL_2}{dt} =& L_2(\mu+\delta) - L_3 f\delta - L_4(1-f)\delta, \\ \frac{dL_3}{dt} =& -A_1 + L_1\left(1-u_1\right)\alpha_1 S - L_2\left(1-u_1\right)\alpha_1 S + L_3\left(d_1 + \eta_1 + \gamma + \mu + \tau(1+u_2)\right) \\ & - L_4\gamma - L_5(\eta_1 + \tau(u_2+1)) - L_6\epsilon_1\left(1-u_1\right), \\ \frac{dL_4}{dt} =& L_4(d_2 + \mu + \theta + \eta_2(u_2+1)) - L_3\theta - A_2 + L_6\epsilon_2(u_1-1) - L_5\eta_2(u_2+1) \\ & - L_1 S\alpha_2(u_1-1) + L_2 S\alpha_2(u_1-1), \\ \frac{dL_5}{dt} =& (\mu+\phi)L_5 - \phi L_1, \\ \frac{dL_6}{dt} =& L_6(\mu_b - r + \chi(u_3+1)) - A_3 - L_1 S\alpha_3(u_1-1) + L_2 S\alpha_3(u_1-1). \end{aligned} \tag{44}$$

with transversality conditions (or final time conditions)

$$L_1(T) = 0, L_2(T) = 0, L_3(T) = 0, L_4(T) = 0, L_5(T) = 0 \text{ and } L_6(T) = 0.$$

The characterizations of the optimal controls $u^*(t)$ and corresponding $u_1^*(t), u_2^*(t), u_3^*(t)$ that is, the optimality equations, are based on the following conditions:

$$\frac{\partial H}{\partial u_1} = \frac{\partial H}{\partial u_2} = \frac{\partial H}{\partial u_3} = 0.$$

where

$$\begin{aligned} \frac{\partial H}{\partial u_1} &= K_1 u_1(t) - L_6(C\epsilon_2 + I\epsilon_1) + L_1 S(B\alpha_3 + C\alpha_2 + I\alpha_1) - L_2 S(B\alpha_3 + C\alpha_2 + I\alpha_1) = 0, \\ \frac{\partial H}{\partial u_2} &= K_2 u_2(t) + L_5(\eta_2 C + \tau I) - \eta_2 C L_4 - \tau I L_3 = 0, \\ \frac{\partial H}{\partial u_3} &= K_3 u_3(t) - \chi B L_6 = 0, \end{aligned} \tag{45}$$

subject to the constraints $0 \le u_1(t) \le u_{1\max}, 0 \le u_2(t) \le u_{2\max}, 0 \le u_3(t) \le u_{3\max}$. Hence, on solving system (45), we have:

$$\begin{aligned} u_1^*(t) &= \frac{CL_6\epsilon_2 + IL_6\epsilon_1 - BL_1S\alpha_3 + BL_2S\alpha_3 - CL_1S\alpha_2 + CL_2S\alpha_2 - IL_1S\alpha_1 + IL_2S\alpha_1}{K_1}, \\ u_2^*(t) &= \frac{CL_4\eta_2 - CL_5\eta_2 + IL_3\tau - IL_5\tau}{K_2}, \\ u_3^*(t) &= \frac{\chi B L_6}{K_3}. \end{aligned} \tag{46}$$

Set $p^* = \frac{CL_6\epsilon_2+IL_6\epsilon_1-BL_1S\alpha_3+BL_2S\alpha_3-CL_1S\alpha_2+CL_2S\alpha_2-IL_1S\alpha_1+IL_2S\alpha_1}{K_1}$. Thus, using the bounds of the control $u_1(t)$, its optimal control is given by

$$u_1^*(t) = \begin{cases} p^*, \text{if } 0 \leq p^* \leq 1, \\ 0, \text{if } p^* \leq 0, \\ 1, p^* \geq 1. \end{cases} \tag{47}$$

Instead, one might express optimal control as

$$u_1^* = \min\Big\{1, \max\{0, p^*\}\Big\}. \tag{48}$$

Also,

$$u_2^*(t) = \begin{cases} \frac{CL_4\eta_2-CL_5\eta_2+IL_3\tau-IL_5\tau}{K_2}, \text{if } 0 \leq \frac{CL_4\eta_2-CL_5\eta_2+IL_3\tau-IL_5\tau}{K_2} \leq 1, \\ 0, \text{if } \frac{CL_4\eta_2-CL_5\eta_2+IL_3\tau-IL_5\tau}{K_2} \leq 0, \\ 1, \text{if } \frac{CL_4\eta_2-CL_5\eta_2+IL_3\tau-IL_5\tau}{K_2} \geq 1. \end{cases} \tag{49}$$

This can also be represented as

$$u_2^* = \min\Big\{1, \max\Big\{0, \frac{CL_4\eta_2 - CL_5\eta_2 + IL_3\tau - IL_5\tau}{K_2}\Big\}\Big\}. \tag{50}$$

Lastly,

$$u_3^*(t) = \begin{cases} \frac{\chi BL_6}{K_3}, 0 \leq \frac{\chi BL_6}{K_3} \leq 1, \\ 0, \text{if } \frac{\chi BL_6}{K_3} \leq 0, \\ 1, \text{if } \frac{\chi BL_6}{K_3} \geq 1. \end{cases} \tag{51}$$

This can also be represented as

$$u_3^* = \min\Big\{1, \max\Big\{0, \frac{\chi BL_6}{K_3}\Big\}\Big\}. \quad \square \tag{52}$$

5. Numerical results

In this section, numerical results for the state system (37) and adjoint system (44) are discussed. The fourth-order Runge–Kutta scheme, also known as RK4, is used to solve the adjoint system due to its reliability compared to Euler's method [30].

RK4 is a convergent numerical method, meaning that as the step size approaches zero, the approximation of the solution becomes more accurate. However, there is a trade-off between computational efficiency and accuracy, as smaller step sizes require more computation time. RK4 is conditionally stable, requiring a sufficiently small step size to remain stable. Smaller step sizes lead to more excellent stability but at the cost of increased computation time. However, RK4 is more stable than lower-order methods like the Euler method. RK4 is also known for its high accuracy, with the error being proportional to the fifth power of the step size.

Generally, the fourth-order Runge–Kutta scheme is a widely used numerical method for solving ODEs, thanks to its convergence, stability, and accuracy. The method is particularly well-suited for solving ODEs with complex behavior but requires a careful choice of step size to balance computational efficiency and accuracy.

The intent of carrying out the numerical solution in this part was to confirm the analytical results achieved in the preceding sections. The scheme was implemented using MATLAB software. Plots of the numerical solution are utilized to evaluate the effectiveness of control efforts on the target population.

5.1. Iterative method

We begin the iterative method by first considering a model without controls; all control variables are set equal to zero; since the adjoint variables depend on the controls, they all also take the value zero. Using the forward-in time Euler's method to Eq. (37), at initial conditions $S(0) = S_0, E(0) = E_0, I(0) = I_0, C(0) = C_0, R(0) = R_0, B(0) = B_0$, some solutions are given as demonstrated in the plots. Also, a forward–backward sweep approach based on the RK4 method [55] was implemented to a set of differential equations with initial conditions and the other with terminal conditions. Interested readers are referred to authors such as [26] for details.

5.2. Control scenarios

Several categories can be established with the discussed controls: those involving a single control, those with two controls, and those with three controls. Thus, seven strategies can be implemented from the three controls considered. The following control schedules were evaluated in order to determine their impact on the elimination of amebiasis:

Strategy A: Control with awareness programs only ($u_1 \neq 0, u_2 = 0, u_3 = 0$)

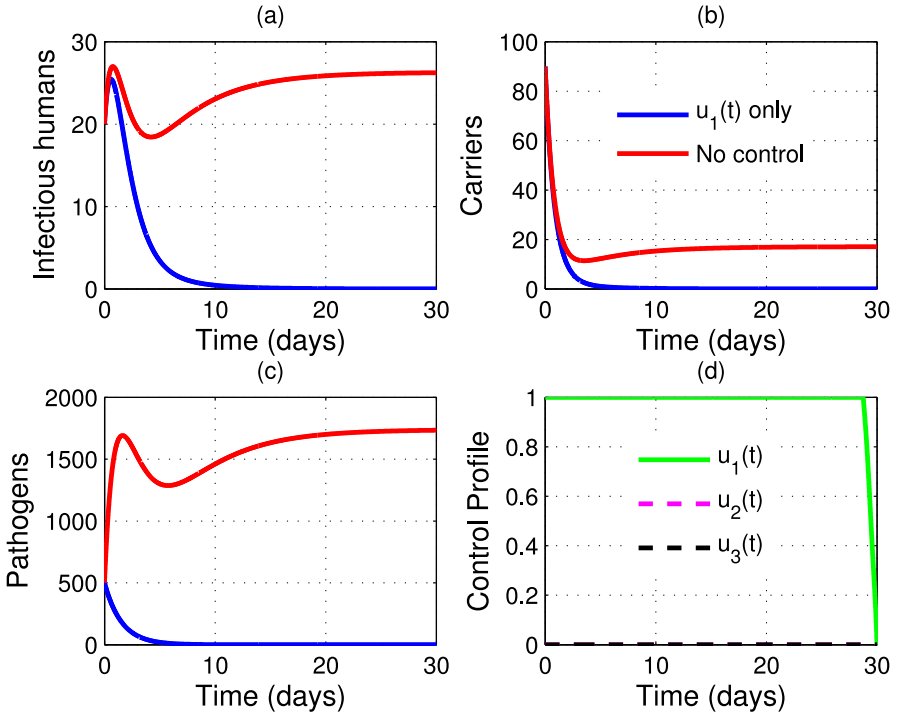

Fig. 3. Effectiveness of awareness programs (u_1) to control amebiasis transmission.

Strategy B: Control with treatment only ($u_1 = 0, u_2 \neq 0, u_3 = 0$)
Strategy C: Control with sanitation only ($u_1 = 0, u_2 = 0, u_3 \neq 0$)
Strategy D: Control with awareness programs and treatment ($u_1 \neq 0, u_2 \neq 0, u_3 = 0$)
Strategy E: Control with awareness programs and sanitation ($u_1 \neq 0, u_2 = 0, u_3 \neq 0$)
Strategy F: Control with treatment and sanitation ($u_1 = 0, u_2 \neq 0, u_3 \neq 0$)
Strategy G: Control with all three controls: awareness programs, treatment, and sanitation ($u_1 \neq 0, u_2 \neq 0, u_3 \neq 0$).

Further, for the simulation purpose of an optimal control problem, these initial values were considered: $S(0) = 20, E(0) = 40, I(0) = 20, C(0) = 90, R(0) = 20$ and $B(0) = 500$. Similarly, the coefficients considered for the state and control variables are $A_1 = 0.4, A_2 = 0.8, A_3 = 0.3, K_1 = 0.1, K_2 = 0.7$ and $K_3 = 0.5$. It should be noted that the weights used in the simulations are entirely hypothetical, as they were intentionally selected to show the optimal control possibilities presented in this article. Likewise, other values used for simulation are $u_1 = u_2 = u_3 = 1$ and $T = 30$ days.

5.2.1. Strategy A: Control with awareness programs only (u_1)

From Fig. 3, treatment control u_2 and sanitation control u_3 are set to zero; thus, the control u_1 optimizes the objective functional (J). It can be seen from Figs. 3(a)–(c) that employing this strategy tends to minimize the number of amebiasis infections greatly. For instance, Fig. 3(a) shows that the number of amebiasis cases can be reduced by using this approach strictly for between 5 and 10 days. From Fig. 3(b), the number of carriers approaches zero on the fifth day. Likewise, it can seen from Fig. 3(c) that applying a similar option will clear the pathogens population on the same fifth day. The results indicate that an awareness program is pivotal to eradicating the disease from the community. The control profile from Fig. 3(d) shows that one requires the control u_1 be kept at maximum (fullest) for the duration of 28.77 days and becomes zero at 30 days to attain the results in Fig. 3(a)–(c) while both u_2 and u_3 are set to zero. This result accords with the results of research by [30,56].

5.2.2. Strategy B: Control with treatment only (u_2)

From Fig. 4, awareness programs control (u_1) and sanitation control (u_3) are set to zero, while treatment control (u_2) is kept active and is employed to optimize the objective functional (J). As a result, we simulated the optimality system with treatment serving as the only possible intervention. Fig. 4(a) illustrates the significant reduction in infectious populations at a particular time after adopting this approach. From Fig. 4(b), however, one can note that there is a negligible decrease in the number of carriers following the application of treatment of carriers. With Fig. 4(c), the pathogen populations are declining after applying the same strategy. One can observe that treatment is vital in diminishing the number of amebiasis cases, even though it is insufficient to bring this disease to an end when considered alone (see also in [30,57]). Thus necessitating other options to work with treatment to contain this disease.

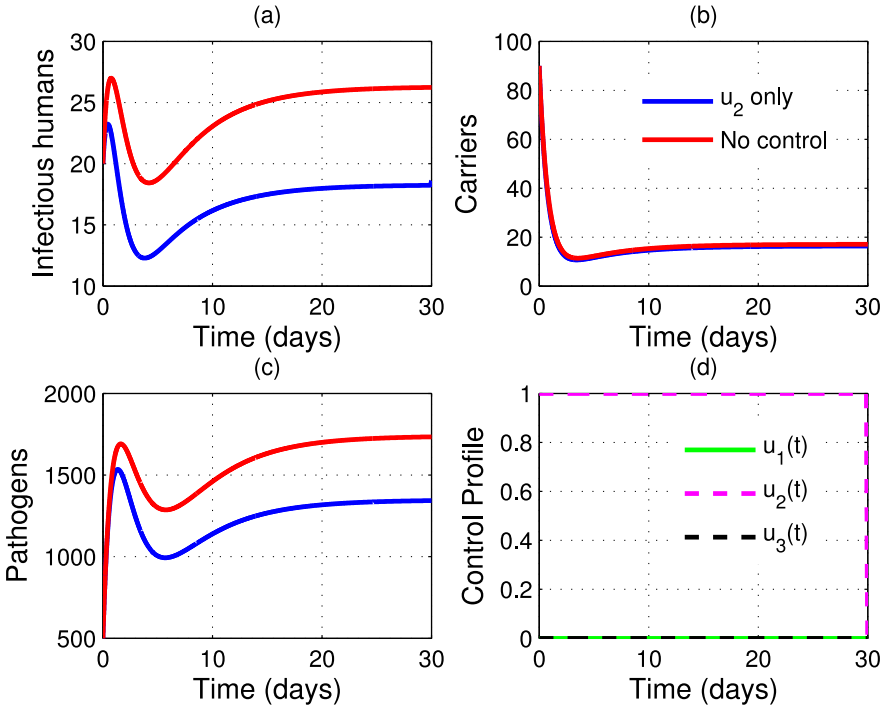

Fig. 4. Impacts of treatment on Amebiasis transmission dynamics.

The control profile from Fig. 4(d) shows that one requires the control u_2 be kept at maximum (fullest) for almost the entire control duration of 30 days to attain the results in Fig. 4(a)–(c) while both u_1 and u_3 are set to zero.

5.2.3. Strategy C: Control with sanitation only (u_3)

From Fig. 5, awareness programs control (u_1) and treatment control (u_2) are set to zero, while sanitation control (u_3) is activated, which is then employed to optimize the objective functional (J). As a result, it can be seen from Fig. 5(a)–(b) that sanitation control has no direct impact on either the number of infectious or carrier populations, respectively. This shows that initiatives like water chlorination and sewage treatment are not intended to eliminate pathogens within diseased people (I and C). Conversely, Fig. 5(c) reveals that sanitation lowers the environmental abundance of amebiasis pathogens. Sanitation practices, including water chlorination, good sewage disposal, and high levels of personal hygiene, all work to limit the spread of amebiasis, which may have sped up this decline. Similarly, the results demonstrate that using this approach alone to combat the disease is ineffective, particularly in areas where it is endemic, necessitating additional strategies to complement sanitation. The control profile from Fig. 5(d) shows that one requires the control u_3 be kept at maximum (fullest) for almost the entire control duration of 30 days to attain the results in Fig. 5(a)–(c) while both u_1 and u_2 are set to zero. A similar conclusion was also seen in [30,57].

5.2.4. Strategy D: Control with awareness campaigns and treatment only (u_1&u_2)

Fig. 6(a) shows that with the application of strategy D, there is a considerable decrease in the number of infectious individuals. Likewise, Fig. 6(b) shows that the carrier population decreases significantly when the same strategy is applied. Note from Fig. 6(c) that the implementation of this strategy also affected the pathogens population. This is because, with this strategy, the number of pathogens concentration tends to reduce substantially. It is interesting to see that the application of this strategy is sufficient to contain the epidemic earlier than 10 days. The control profile from Fig. 6(d) shows that one requires the control u_1 and u_2 be kept at maximum (fullest) for 28.77 days and 3.4 days, respectively. Later, the same control profile drops to zero in 25 and 30 days in the same order to attain the results in Fig. 6(a)–(c) while the control u_3 is set to zero. This finding also agrees with similar works by [30,58].

5.2.5. Strategy E: Control with sanitation and awareness programs only (u_1&u_3)

It can be seen from Fig. 7(a)–(c) that with the application of strategy E, there is a dramatic decrease in the number of the infectious, carrier, and amebiasis pathogens population at a given time. The disease-free state is attained at the 10th day, see Figs. 7(a). Also, the disease-free state for carriers and pathogens is attained earlier than five days (Figs. 7(b-c)). This implies that sanitation and awareness programs can better control amebiasis infections. A similar conclusion was also observed in [30,59,60].

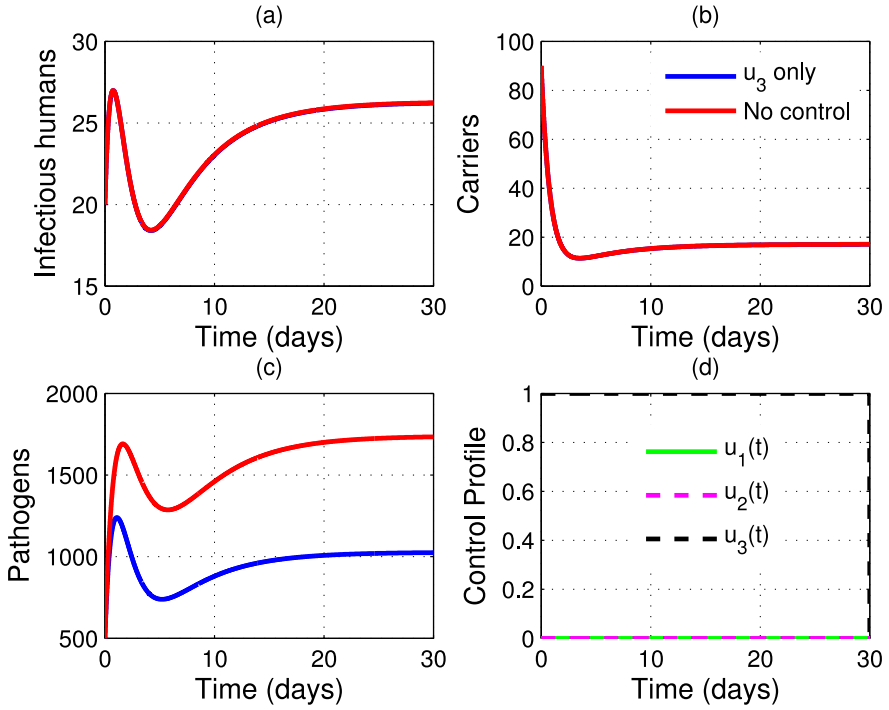

Fig. 5. Impacts of sanitation on amebiasis transmission dynamics.

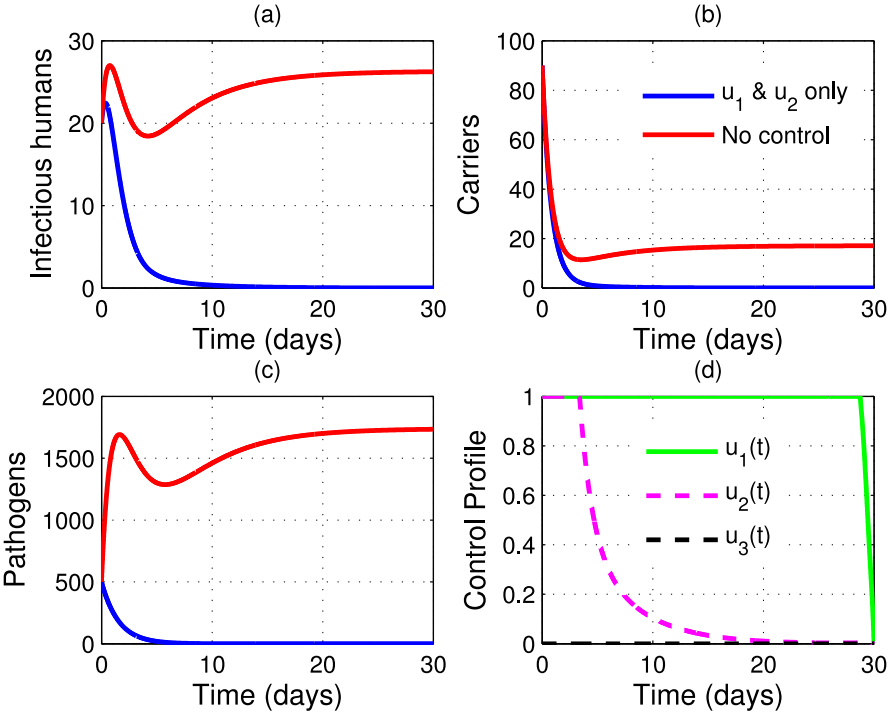

Fig. 6. Impacts of awareness programs and treatment on amebiasis transmission dynamics.

5.2.6. Strategy F: Control with treatment and sanitation only (u_2&u_3)

It can be seen from Fig. 8(a,c) that with the application of strategy F, there is a decrease in the number of infectious and pathogens populations at a given time. Additionally, it is seen from Fig. 8(b) that this strategy has a negligible effect on the carriers. Total

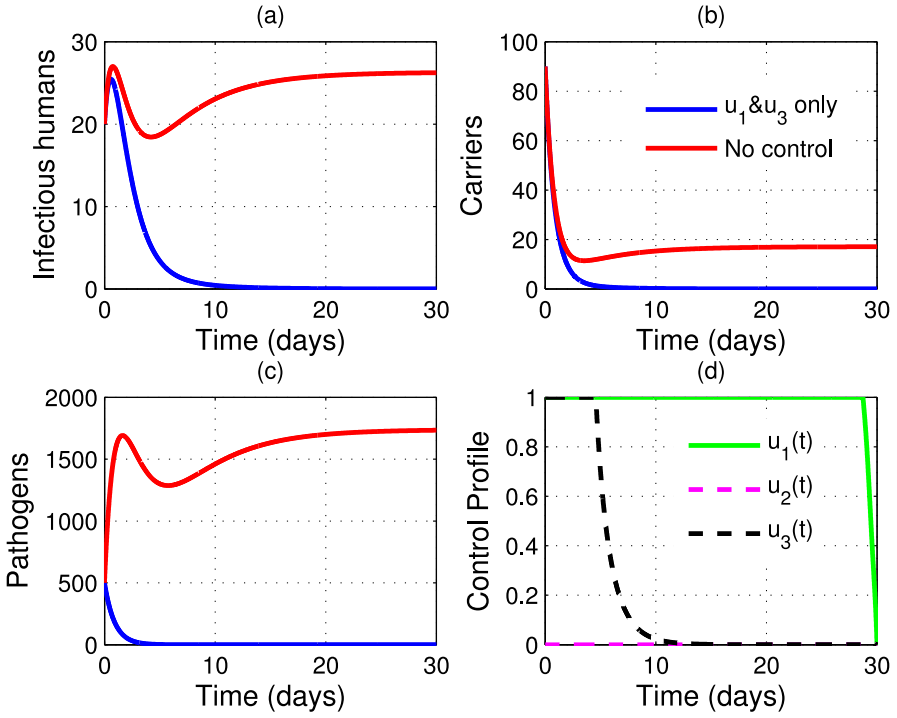

Fig. 7. Impacts of sanitation and awareness program on amebiasis transmission dynamics.

clearing of amebiasis infections cannot be witnessed in Fig. 8(a,c). This implies that sanitation and treatment alone are insufficient to eliminate the disease from the community; other combinations are needed to bring the disease to an end. This finding coincides with those by [30,57].

The control profile from Fig. 8(d) shows that one requires the control u_2 and u_3 be kept at maximum (fullest) for almost the entire control duration of 30 days to attain the results in Fig. 5(a)–(c) while u_1 is set to zero.

5.2.7. Strategy G: Control with treatment, sanitation and awareness programs ($u_1, u_2 \& u_3$)

Fig. 9(a)–(b) shows that the number of infectious and carrier populations at any given period significantly decreases with the implementation of strategy G. Similarly, from Fig. 9(c), it is noticeable that utilizing this approach works best for eliminating amebiasis germs. This finding is more optimistic than when the same controls were considered separately or combined with another strategy, except for treatment and awareness programs, which produce almost identical results. This result highlights the advantages of using multiple controls to eliminate amebiasis infections.

The optimal control profile for attaining the results presented under this strategy is shown in Fig. 9(d), where the control u_1 remains constant for about 28.77 days and becomes zero at 30 days, while the control u_2 remain constant for about 3.49 days and becomes zero at 23.32 days, whereas, the control u_3 remain constant for about 4.59 days and becomes zero at 14.93 days.

The results show that to eliminate this epidemic from the community, one should continually combine treatment, sanitation efforts, and awareness programs in the stated schedule. Medical doses should be kept at maximum initially and be reduced gradually as time goes on to reduce costs and associated side effects. The same applies to sanitation programs, which are applied maximum initially and drop gradually with time. Awareness programs should be maintained high for almost the time control period. A similar conclusion was also seen in [30].

6. Conclusions

In this work, deterministic mathematical models were developed to account for direct and indirect amebiasis transmission. The first model includes two measures: sanitation and treatment. The effective reproduction number was determined using the next-generation matrix approach, and the stability of the equilibria was verified. The Disease-Free Equilibrium (DFE) has been demonstrated to be both locally and globally stable if $R_e < 1$ and unstable otherwise. A sensitivity analysis determined which disease dynamics parameters are crucial and may necessitate additional control measures. It was found that the parameters $\mu, \Lambda, \alpha_3, \mu_b$, and ϵ_1 a are much more sensitive to the effective reproduction number; thus, even a small change in these parameters could significantly impact disease dynamics. It was realized that investing more in implementing sanitation and treatment control measures reduces amebiasis incidence. Indirect transmission contributes to a more significant number of infections than direct transmission. Likewise,

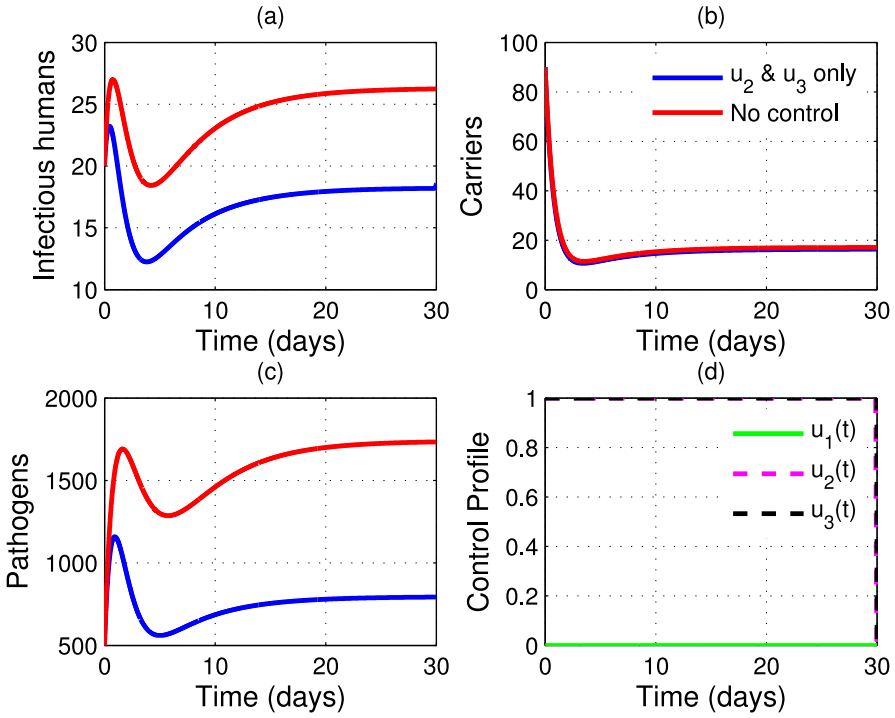

Fig. 8. Impacts of treatment and sanitation on amebiasis transmission dynamics.

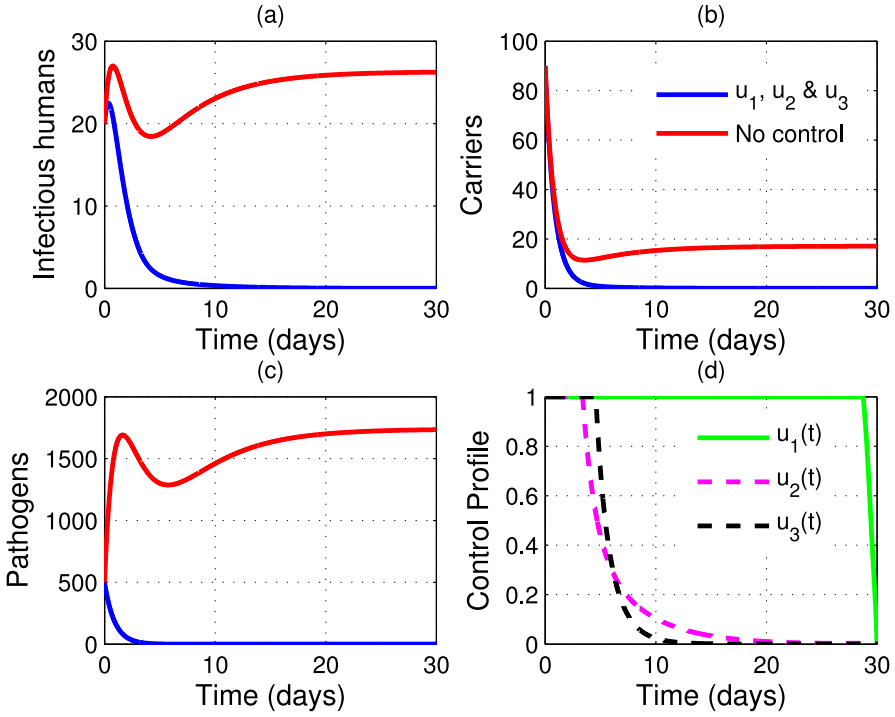

Fig. 9. Impacts of awareness programs, treatment, and sanitation on amebiasis transmission dynamics.

an optimal control problem for amebiasis was formulated. The model has incorporated three optimal controls: awareness programs, treatment, and sanitation. The optimal control model was analyzed via Pontryagin's maximum principle. Numerical simulation was carried out for an optimal control problem to verify analytical results. The findings show that the optimal control strategy combines three controls: awareness programs, treatment, and sanitation. However, a single strategy might be opted for during an economic crisis. In that case, a strategy that considers only awareness programs might be viable to control the epidemic. The authors acknowledge the models presented in the study have limitations and suggest that future work could extend the model to include an age-structured population. This would provide a more realistic representation of the disease's dynamics, as infections may vary among age groups. Moreover, a cost-effectiveness analysis could be done to figure out the most cost-effective strategy. However, the study's findings have important implications for policymakers and public health officials who seek to design effective strategies for controlling amebiasis in the community. The study provides valuable insights into the relative effectiveness of different control measures and can help guide decisions regarding resource allocation for disease control.

Funding

This work did not receive any financial grants.

CRediT authorship contribution statement

Stephen Edward: Conceptualization, Methodology, Software, Data curation, Writing – original draft. **Godfrey Edward Mpogolo:** Software, Validation, Writing – review & editing, Visualization, Investigation.

Declaration of competing interest

The authors declare that they have no competing interests.

Data availability

Data will be made available on request.

Acknowledgments

The authors, SE and GE, thank the University of Dodoma and Tanzania Institute of Accountancy, respectively, for offering the conducive environments to conduct this study.

References

[1] Haque R, Ali IM, Petri Jr WA. Prevalence and immune response to entamoeba histolytica infection in preschool children in Bangladesh. Am J Trop Med Hygiene 1999;60(6):1031–4.
[2] Clark CG, Diamond LS. The Laredo strain and other 'Entamoeba histolytica-like'amoebae are Entamoeba moshkovskii. Mol Biochem Parasitol 1991;46(1):11–8.
[3] Stauffer W, Ravdin JI. Entamoeba histolytica: an update. Curr Opin Infect Dis 2003;16(5):479–85.
[4] Ximénez C, Morán P, Rojas L, Valadez A, Gómez A. Reassessment of the epidemiology of amebiasis: State of the art. Inf Genet Evol 2009;9(6):1023–32.
[5] Fathi AM, Bahnass MM, Elshahawy IS. Short communication seroprevalence of amoebiasis in Najran Saudi Arabia. Trop Biomed 2017;34(3):732–40.
[6] Samie A, ElBakri A, AbuOdeh RE. Amoebiasis in the tropics: Epidemiology and pathogenesis. Curr Top Trop Med 2012;201.
[7] CC S, Saha S, Raychoudhury V, Fidele H, Sinha S. CISER: An amoebiasis-inspired model for Epidemic Message Propagation in DTN. 2016, arXiv preprint arXiv:1608.07670.
[8] Fotedar R, Stark D, Beebe N, Marriott D, Ellis J, Harkness J. Laboratory diagnostic techniques for Entamoeba species. Clin Microbiol Rev 2007;20(3):511–32.
[9] Hertz R, Ben Lulu S, Shahi P, Trebicz-Geffen M, Benhar M, Ankri S. Proteomic identification of S-nitrosylated proteins in the parasite Entamoeba histolytica by resin-assisted capture: insights into regulating the Gal/GalNAc lectin by nitric oxide. PLoS One 2014;9(3):e91518.
[10] Bansal D, Malla N, Mahajan RC. Drug resistance in amoebiasis. Indian J Med Res 2006;123(2):115.
[11] Quach J, St-Pierre J, Chadee K. The future for vaccine development against Entamoeba histolytica. Hum Vacc Immunotherapeut 2014;10(6):1514–21.
[12] Hategekimana F, Saha S, Chaturvedi A. Amoebiasis Transmission and Life cycle: A continuous state description by existence and uniqueness. Glob J Pure Appl Math 2016;12(1):375–90.
[13] Hategekimana F, Saha S, Chaturvedi A. Dynamics of amoebiasis transmission: stability and sensitivity analysis. Mathematics 2017;5(4):58.
[14] Lenhart S, Workman JT. Optimal control applied to biological models. CRC press; 2007.
[15] Kwasi-Do Ohene Opoku N, Afriyie C. The role of control measures and the environment in the transmission dynamics of cholera. In: Abstract and applied analysis. Vol. 2020. Hindawi; 2020.
[16] Omame A, Okuonghae D. A co-infection model for oncogenic Human papillomavirus and tuberculosis with optimal control and cost-effectiveness analysis. Optim Control Appl Methods 2021;42(4):1081–101.
[17] Omame A, Abbas M, Onyenegecha CP. Backward bifurcation and optimal control in a co-infection model for SARS-CoV-2 and ZIKV. Results Phys 2022;37:105481.
[18] Omame A, Okuonghae D, Nwafor UE, Odionyenma BU. A co-infection model for HPV and syphilis with optimal control and cost-effectiveness analysis. Int J Biomathemat 2021;14(07):2150050.
[19] Omame A, Isah ME, Abbas M. An optimal control model for COVID-19, Zika, Dengue, and Chikungunya co-dynamics with reinfection. Opt Control Appl Methods 2023;44(1):170–204.
[20] Abidemi A, Olaniyi S, Adepoju OA. An explicit note on the existence theorem of optimal control problem. J Phys Conf Ser 2022;2199:012021.

[21] Olaniyi S, Falowo OD, Okosun KO, Mukamuri M, Obabiyi OS, Adepoju OA. Effect of saturated treatment on malaria spread with optimal intervention. Alexandria Eng J 2023;65:443–59.
[22] Olaniyi S, Mukamuri M, Okosun KO, Adepoju OA. Mathematical analysis of a social hierarchy-structured model for malaria transmission dynamics. Results Phys 2022;34:104991.
[23] Bakhtiar T. Optimal intervention strategies for cholera outbreak by education and chlorination. In: IOP conference series: Earth and environmental science. Vol. 31. No. 1. IOP Publishing; 2016, 012022.
[24] Wang J, Modnak C. Canad. App Math Quart 2011;19(3):255–73.
[25] Berhe HW, Makinde OD, Theuri DM. Parameter estimation and sensitivity analysis of dysentery diarrhea epidemic model. J Appl Math 2019;2019.
[26] Mwaijande SE, Mpogolo GE. Mathematical modeling of the transmission dynamics of amebiasis with some interventions. 2022, Researchsquare [Preprint]. March 3, [Accessed 19 October 2022]. Available from: http://dx.doi.org/10.21203/rs.3.rs-1363033/v1.
[27] Haque R, Mondal D, Duggal P, Kabir M, Roy S, Farr BM, et al. Entamoeba histolytica infection in children and protection from subsequent amebiasis. Inf Immun 2006;74(2):904–9.
[28] Blessmann J, Ali IKM, Ton Nu PA, Dinh BT, Ngo Viet TQ, Le Van A, et al. Longitudinal study of intestinal Entamoeba histolytica infections in asymptomatic adult carriers. J Clin Microbiol 2003;41(10):4745–50.
[29] Gathiram V, Jackson TFHG. A longitudinal study of asymptomatic carriers of pathogenic zymodemes of Entamoeba histolytica. South Afr Med J 1987;72(10):669–72.
[30] Edward S, Shaban N, Mureithi E. Optimal control of shigellosis with cost-effective strategies. Comput Math Methods Med 2020;2020.
[31] Keeling Matt J, Pejna Rohani. Modelling infectious diseases in humans and animals. 2008, Princeton University Press; 2007.
[32] Petri Jr WA, Singh U. Diagnosis and management of amebiasis. Clin Inf Dis 1999;1117–25.
[33] Edward S, Mureithi E, Shaban N. Shigellosis dynamics: Modelling the effects of treatment, sanitation, and education in the presence of carriers. Int J Math Math Sci 2020;2020.
[34] Abd-Alla MD, Jackson TF, Rogers T, Reddy S, Ravdin JI. Mucosal immunity to asymptomatic Entamoeba histolytica and Entamoeba dispar infection is associated with a peak intestinal anti-lectin immunoglobulin A antibody response. Inf Immun 2006;74(7):3897–903.
[35] Birkhoff G, Rota GC. Ordinary differential equation. Ginn. and Co. Boston; 1982;
[18], May RM. Stability and Complexity in Model Ecosystems. 2001.
[36] Batista M. On the reproduction number in epidemics. J Biol Dyn 2021;15(1):623–34.
[37] Driessche PVD, Watmough J. Further notes on the basic reproduction number. In: Mathematical epidemiology. Berlin, Heidelberg: Springer; 2003, p. 159–78.
[38] Diekmann O, Heesterbeek JAP, Roberts MG. The construction of next-generation matrices for compartmental epidemic models. J R Soc Interface 2009;7(47):873–85.
[39] DeJesus EX, Kaufman C. Routh–Hurwitz criterion in the examination of eigenvalues of a system of nonlinear ordinary differential equations. Phys Rev A 1987;35(12):5288.
[40] Morris J. The Routh and Routh–Hurwitz stability criteria: Their derivation by a novel method using comparatively elementary algebra. Aircraft Eng Aerospace Technol 1962;34(1):25–7.
[41] McNabb A. Comparison theorems for differential equations. J Math Anal Appl 1986;119(1-2):417–28.
[42] Chitnis N, Hyman JM, Cushing JM. Determining important parameters in the spread of malaria through the sensitivity analysis of a mathematical model. Bull Math Biol 2008;70(5):1272.
[43] Haque R, Huston CD, Hughes M, Houpt E, Petri WA. Amebiasis. New England J Med 2003;348(16):1565–73.
[44] Shekhar S, Xiong H, editors. Encyclopedia of GIS. Springer Science & Business Media; 2007.
[45] Marino S, Hogue IB, Ray CJ, Kirschner DE. A methodology for performing global uncertainty and sensitivity analysis in systems biology. J Theor Biol 2008;254(1):178–96.
[46] Berhe HW, Makinde OD, Theuri DM. Optimal control and cost-effectiveness analysis for dysentery epidemic model. Appl Math Inf Sci 2018;12:1183–95.
[47] Falowo OD, Olaniyi S, Oladipo AT. Optimal control assessment of Rift Valley fever model with vaccination and environmental sanitation in the presence of treatment delay. Model Earth Syst Environ 2023;9(1):457–71.
[48] Jung E, Lenhart S, Feng Z. Optimal control of treatments in a two-strain tuberculosis model. Discrete Continuous Dyn Syst-B 2002;2(4):473.
[49] Kern DL, Lenhart S, Miller R, Yong J. Optimal control applied to native–invasive population dynamics. J Biol Dyn 2007;1(4):413–26.
[50] Joshi HR. Optimal control of an HIV immunology model. Opt Control Appl Methods 2002;23(4):199–213.
[51] Laarabi H, Abta A, Hattaf K. Optimal control of a delayed SIRS epidemic model with vaccination and treatment. Acta Biotheoretica 2015;63(2):87–97.
[52] Gumel AB, Castillo-Chávez C, Mickens RE, Clemence DP, editors. Mathematical studies on human disease dynamics: Emerging paradigms and challenges: AMS-IMS-SIAM joint summer research conference on modeling the dynamics of human diseases: Emerging paradigms and challenges. Vol. 410. Snowbird, Utah: American Mathematical Soc; 2006, p. 17–21, 2005.
[53] Lukes DL. Differential equations: Classical to controlled. New York: Academic Press; 1982.
[54] Fleming WH, Rishel RW. Deterministic and stochastic optimal control. New York: Springer; 1975.
[55] Pontryagin LS, Boltyanskii VG, Gamkrelidze RV, Mishchenko EF. The mathematical theory of optimal processes. Hoboken, NJ, USA: JohnWiley & Sons; 1962.
[56] Misra AK, Sharma A, Shukla JB. Stability analysis and optimal control of an epidemic model with awareness programs by media. Biosystems 2015;138:53–62.
[57] Tilahun GT, Makinde OD, Malonza D. Modelling and optimal control of typhoid fever disease with cost-effective strategies. Comput Math Methods Med 2017;2017.
[58] Panja P. Optimal control analysis of a cholera epidemic model. Biophys Rev Lett 2019;14(01):27–48.
[59] Rai RK, Misra AK, Takeuchi Y. Modelling the impact of sanitation and awareness on the spread of infectious diseases. Math Biosci Eng 2019;16(2):667–700.
[60] Mwasa A, Tchuenche JM. Mathematical analysis of a cholera model with public health interventions. Biosystems 2011;105(3):190–200.